

Tracing metal sources for the giant McArthur River Zn-Pb deposit (Australia) using lead isotopes

Joséphine Gigon^{1*}, Etienne Deloule², Julien Mercadier¹, David L. Huston³, Antonin Richard¹, Irvine R. Annesley¹, Andrew S. Wygralak⁴, Roger G. Skirrow³, Terrence P. Mernagh⁵ and Kristian Masterman⁶

¹Université de Lorraine, CNRS, GeoRessources, Campus Aiguillettes, rue Jacques Callot BP 70239, 54506 Vandœuvre-lès-Nancy, France

²Centre de Recherches Péetrographiques et Géochimiques (CRPG), UMR 7358 CNRS-UL, 15 rue Notre Dame des Pauvres, F-54501 Vandœuvre-lès-Nancy, France

³Geoscience Australia, GPO Box 378, Canberra, ACT 2601, Australia

⁴Northern Territory Geological Survey, PO Box 2901, Darwin, NT 0801, Australia

⁵Research School of Earth Sciences, Australian National University, Acton, ACT2601, Australia

⁶Glencore Australia Holdings Pty Ltd, 1 Macquarie Place, Sydney, NSW2000, Australia

ABSTRACT

Giant hydrothermal ore deposits form where fluids carrying massive amounts of metals scavenged from source rocks or magmas encounter conditions favorable for their localized deposition. However, in most cases, the ultimate origin of metals remains highly disputed. Here, we show for the first time that two metal sources have provided, in comparable amounts, the 8 Mt of lead of the giant McArthur River zinc-lead deposit (McArthur Basin, Northern Territory, Australia). By using high-resolution secondary ion mass spectrometry (SIMS) analysis of lead isotopes in galena, we demonstrate that the two metal sources were repeatedly involved in the metal deposition in the different ore lenses ca. 1640 Ma. Modeling of lead isotope fractionation between mantle and crustal reservoirs implicates felsic rocks of the crystalline basement and the derived sedimentary rocks in the basin as the main lead sources that were leached by the ore-forming fluids. This sheds light on the crucial importance of metal tracing as a prerequisite to constrain large-scale ore-forming systems, and calls for a paradigm shift in the way hydrothermal systems form giant ore deposits: leaching of metals from several sources may be key in accounting for their huge metal tonnage.

INTRODUCTION

More than a thousand giant ore deposits worldwide are recognized as containing exceptional accumulations of metals in restricted volumes (i.e., they store the metals equivalent in 10^{11} tons of continental crust in mean crustal or “Clarke” concentration; Laznicka, 2014). Hydrothermal ore deposits are a specific class of metallic deposits that form by a combination of (1) metal extraction from a source rock or magma by a hydrothermal fluid, (2) metal transport by a hydrothermal fluid from the source to a focused discharge where metals precipitate and accumulate, and (3) metal precipitation and accumulation (e.g., McCuaig and Hronsky, 2014).

Giant hydrothermal ore deposits form only when all of these processes are adequately combined in space and time (e.g., Richards, 2013) and when the volume of metalliferous fluid is sufficient. While the conditions for metal transport and precipitation are relatively well understood, thanks to, among others, fluid inclusion studies and metal speciation and mineral solubility experiments (e.g., Richard et al., 2012), the conditions under which metals are extracted from their source, and more specifically the nature of the metal sources, are still the most disputed aspect of many ore-deposit models (e.g., Pettke et al., 2010). Several factors may underlie this controversy: (1) metal sources may occur at great distance from the ore deposit and may be hidden (e.g., Harlaux et al., 2018); (2) metal

sources typically have large volumes but low concentrations of metal, meaning that the mass-balance studies required to demonstrate large-scale metal mobilization are highly challenging (e.g., Pitcairn et al., 2006); (3) a single ore deposit may form from several metal sources (e.g., Mercadier et al., 2013); and (4) fluid mixing may play a role in subsequent dilution of the geochemical signature of the primary metal source(s).

In order to address the number and the nature of metal source(s) involved with the formation of a true giant hydrothermal ore deposit, we have targeted the McArthur River zinc-lead deposit (Northern Territory, Australia) and carried out a detailed *in situ* Pb isotope study of galena. This widely used method is a powerful tool for tracing metal sources and ages based on model ages because it combines three radioactive decay systems ($^{238}\text{U} \rightarrow ^{206}\text{Pb}$, $^{235}\text{U} \rightarrow ^{207}\text{Pb}$, and $^{232}\text{Th} \rightarrow ^{208}\text{Pb}$; e.g., Deloule et al., 1986).

GEOLOGICAL SETTING

The McArthur River Zn-Pb deposit is one of many giant hydrothermal ore deposits of the sediment-hosted massive sulfide (SHMS) category (e.g., Large et al., 1998; Leach et al., 2010). This deposit is situated in the Paleoproterozoic to Mesoproterozoic McArthur Basin, which unconformably overlies Paleoproterozoic crystalline basement units (Fig. 1; Fig. DR1 in the GSA Data Repository¹). This is one of the many giant ore deposits of the so-called

*E-mail: josephine.gigon@gmail.com

¹GSA Data Repository item 2020140, description of the parameters used for optical and scanning electron microscopy and secondary ion mass spectrometry; an extended discussion and an explanation of the different models presented in the main text; data tables; and supplemental figures, is available online at <http://www.geosociety.org/datarepository/2020/>, or on request from editing@geosociety.org.

CITATION: Gigon, J., et al., 2020, Tracing metal sources for the giant McArthur River Zn-Pb deposit (Australia) using lead isotopes: *Geology*, v. 48, p. 478–482, <https://doi.org/10.1130/G47001.1>

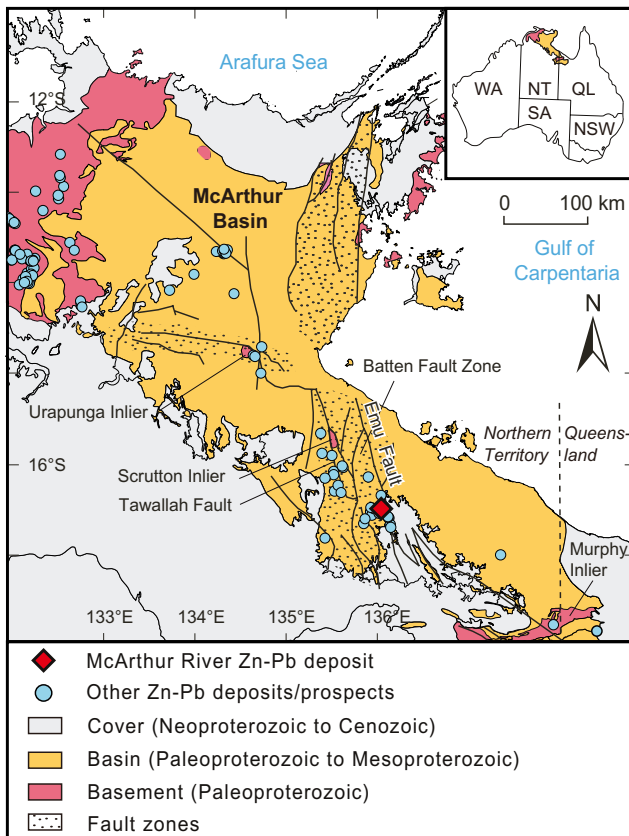


Figure 1. Simplified geological map of McArthur Basin (Northern Territory, Australia), with identification of major lithostratigraphic units: crystalline basement, McArthur Basin, and more recent sedimentary cover (Ahmad et al., 2013). Major faults and fault zones are indicated, including the Emu fault near the McArthur River Zn-Pb deposit. Other Zn-Pb deposits and prospects are indicated. WA—Western Australia; NT—Northern Territory; QL—Queensland; SA—South Australia; NSW—New South Wales.

“Carpentaria zinc belt” in the Northern Territory and Queensland (Large et al., 1998; McGoldrick et al., 2010) and one of the most important Zn-Pb deposits in the world (as of June 2019: 172 Mt at 9.9% Zn, 4.6% Pb, 47 g/t Ag; NTGS, 2019). The McArthur River deposit is located 2 km west of the Emu fault, a major 10-km-deep crustal structure (Rawlings et al., 2004) that potentially acted as a fluid conduit for upward migration of 150–250 °C, oxidized, metal- and sulfate-rich basal fluids (Cooke et al., 2000) in a sinistral strike-slip regime (McGoldrick et al., 2010). The eight ore lenses of the McArthur River deposit occur within the Pyritic Shale Member of the Barney Creek Formation, dated at 1639 ± 2 Ma (Page and Sweet, 1998), which acted as a reduced geochemical trap for metal precipitation (Cooke et al., 2000). Most authors consider the formation of the McArthur River deposit as syn-sedimentary or sub-contemporaneous to the deposition of the upper Barney Creek Formation, and therefore consider 1639 ± 2 Ma as a reasonable estimate of the age of metal deposition (Huston et al., 2006; Kunzmann et al., 2019).

SAMPLING AND ANALYTICAL METHODS

Samples span most of the ore sequence at the McArthur River mine site (16.436° S, 136.098° E, Geocentric Datum of Australia 1994) and are from four of the eight ore lenses and so-called

lenses 0 and 9, two sub-economic lenses located just below and above the main ore sequence, respectively (Fig. 2). Petrographic investigation by reflected-light optical microscopy and scanning electron microscopy (SEM) shows that ores consist of sphalerite-galena-pyrite-rich bands interlayered with mudstones and quartz-carbonate turbidites (Fig. 2; Large et al., 1998). Galena crystals 50 μ m to 1 mm in size are typically poikilitic and contain numerous ~ 10 μ m inclusions of pyrite, sphalerite, and minor silicates and carbonates. No growth, recrystallization, zoning, or alteration textures in galena were highlighted. Detailed mineral mapping using SEM was carried out in order to select the most favorable zones within galena grains (i.e., galena devoid of mineral inclusions) for *in situ* Pb isotope analyses. The lead isotopes were measured by secondary ion mass spectrometry (SIMS) with a radiofrequency source whose analytical capacity allows an excellent sensitivity and a high spatial resolution with a spot size of 10 μ m. Analytical methods are detailed in the Data Repository.

RESULTS

The ranges of $^{206}\text{Pb}/^{204}\text{Pb}$, $^{207}\text{Pb}/^{204}\text{Pb}$, and $^{208}\text{Pb}/^{204}\text{Pb}$ ratios are 16.10–16.22, 15.43–15.57, and 35.42–36.57 respectively (Fig. 3; Table DR1). In a $^{207}\text{Pb}/^{204}\text{Pb}$ versus $^{206}\text{Pb}/^{204}\text{Pb}$ diagram, the data are distributed along a line whose slope is 1.42 with a mean square weighted devi-

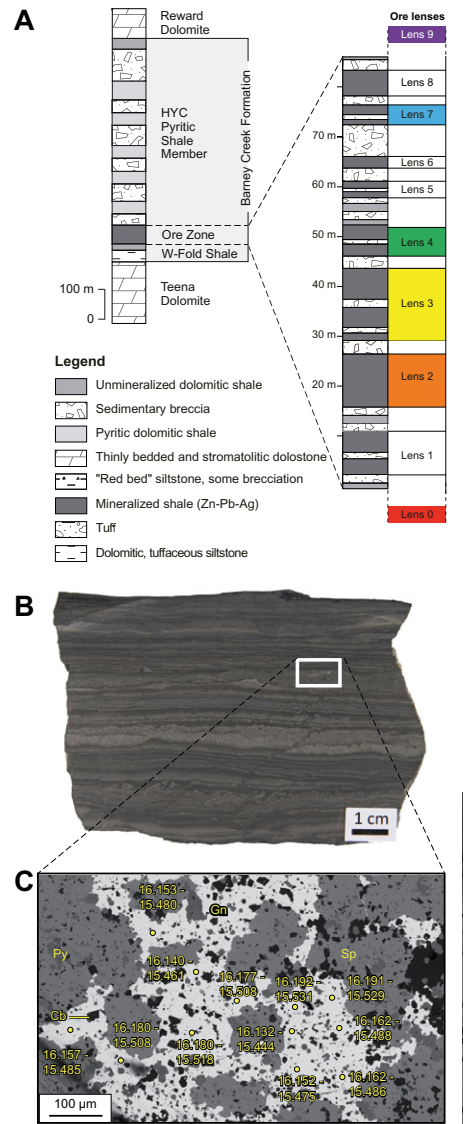


Figure 2. Stratigraphy of sample location in the McArthur River Zn-Pb deposit (Northern Territory, Australia) and description of a typical sample. (A) Simplified stratigraphic succession of the McArthur River deposit with locations of different ore lenses (Large et al., 1998). Sampled ore lenses (0, 2, 3, 4, 7, and 9) are identified by different colors. (B) Hand sample from lens 2 with sulfide-rich laminae. (C) Backscattered electron scanning microscopy image of sulfide-rich lamina showing texture of galena (Gn, white), sphalerite (Sp, light gray), pyrite (Py, dark gray), and carbonate (Cb, black) and size and emplacement of *in situ* Pb isotope analyses by secondary ion mass spectrometry (SIMS). For each SIMS spot, Pb isotopic ratios are indicated as follows: $^{206}\text{Pb}/^{204}\text{Pb}$ - $^{207}\text{Pb}/^{204}\text{Pb}$.

ation (MSWD) of 4.1 (Fig. 3). Slopes are similar within the analytical error for the different lenses (Fig. DR2). Lenses 0, 3, 4, and 9 show a similar distribution of $^{206}\text{Pb}/^{204}\text{Pb}$ and $^{207}\text{Pb}/^{204}\text{Pb}$ ratios with modes around 16.2 and 15.55 respectively, whereas lens 2 shows modes around 16.16 and 15.49, respectively. The Pb isotope

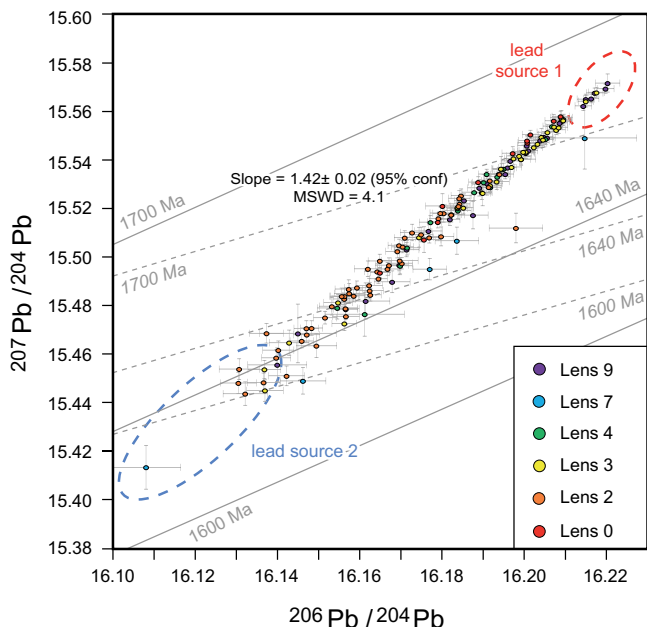


Figure 3. Lead isotope composition of galena from the McArthur River Zn-Pb deposit (Northern Territory, Australia). *In situ* secondary ion mass spectrometry data from different ore lenses are identified by distinct colors as in Figure 2, and plotted with 1 σ error bars. Slope of line along which all analyses plot and position of ellipses corresponding to the probable ratios of lead sources 1 and 2 are shown (conf—confidence; MSWD—mean square weighted deviation). Isochrons (straight lines linking compositions of rocks or minerals having same model age) from different models (solid lines: Sun et al., 1996, dashed lines: Stacey and Kramers, 1975) are indicated.

ratios exhibit similar variations at the grain and lens scales (e.g., $^{206}\text{Pb}/^{204}\text{Pb}$ values of 16.192 and 16.132 for analytical spots 100 μm apart in a single grain; Figs. DR3–DR8). Previous Pb isotope compositions measured on mixed sulfides by thermal ionization mass spectrometry (TIMS) are clustered in the lower range of the $^{206}\text{Pb}/^{204}\text{Pb}$, $^{207}\text{Pb}/^{204}\text{Pb}$, and $^{208}\text{Pb}/^{204}\text{Pb}$ values obtained in this study (Fig. DR9). Although they are compatible within error with the present data, they represent a mixed signature of several grains. The novelty here is that the *in situ* SIMS analyses have a high petrographic resolution and reveal the full range of Pb isotope compositions.

DISCUSSION

Repeated Mixing between Two Lead Sources

The line along which all of the lead isotope data are distributed is discordant to isochrons linking rocks and minerals with the same model age (Fig. 3; Stacey and Kramers, 1975; Sun et al., 1996). The most simple explanation is that the data lie along a mixing line between two distinct Pb sources corresponding to two end members of the data distribution that we name, respectively, lead source 1 ($^{207}\text{Pb}/^{204}\text{Pb} > 15.56$ and $^{206}\text{Pb}/^{204}\text{Pb} > 16.21$) and lead source 2 ($^{207}\text{Pb}/^{204}\text{Pb} < 15.46$ and $^{206}\text{Pb}/^{204}\text{Pb} < 16.14$; Fig. 3). Assuming that (1) the two lead sources have compositions similar to those of the extremes of the mixing line and (2) the data are representative of the Pb isotopic composition of the ore fluid at the time of sulfide deposition, the relative contributions from the two sources can be calculated. Considering the modes of $^{207}\text{Pb}/^{204}\text{Pb}$ and $^{206}\text{Pb}/^{204}\text{Pb}$ ratios in each lens,

the relative proportion of Pb derived from each source in the different ore lenses is between 38% and 83% for lead source 1 and between 17% and 62% for lead source 2 (Fig. DR2). Thus, both Pb sources have been repeatedly involved in the formation of the different ore lenses, and their relative proportions are of the same order of magnitude.

Isotope Evolution Models for Lead Sources

Models of Pb lead isotope fractionation and evolution between the mantle and crustal reservoirs, together with existing chronostratigraphic constraints in the investigated area, are helpful in identifying the nature of lead sources 1 and 2. The usual local model for the North Australian craton is based on the global “continuous growth-of- μ ” model (where μ represents the $^{238}\text{U}/^{204}\text{Pb}$ ratio of a given reservoir; Cumming and Richards, 1975), and uses Pb isotope ratios obtained by TIMS at the McArthur River deposit as a control point for the 1640 Ma isochron (Fig. DR9; Sun et al., 1996). However, because the new *in situ* SIMS data presented here show considerably more scattering compared to previously obtained bulk TIMS data, the local model should now be treated with caution. Alternative models are proposed and discussed below (see Fig. 4, and the Data Repository, for details).

The objective of the tested models is to account for distinct evolution of lead sources 1 and 2 which were both leached by the ore-forming fluids at ca. 1640 Ma, by adjusting the number and timing of crust formation and differentiation events, the age of crystallization of Pb-bearing minerals, as well as the μ values of the different Pb reservoirs. Because the composition of

lead source 2 lies close to the 1640 Ma isochron of the usual global and local models (Fig. 3; Stacey and Kramers, 1975; Sun et al., 1996), we rely on the reasonable assumption that lead source 2 corresponds to a crustal reservoir that has evolved isotopically through ^{238}U , ^{235}U , and ^{232}Th decay until the time of the McArthur River deposit formation (ca. 1640 Ma). Model A assumes that the model age of both lead sources is 1640 Ma. Back-calculation indicates the extraction of a crustal reservoir from the mantle at 3.83 Ga that evolved toward the composition of lead source 1 ($\mu_1 = 10.21$), followed at 3.65 Ga by the extraction of another crustal reservoir from the mantle that evolved toward the composition of lead source 2 ($\mu_2 = 10.34$; Fig. 4A). Model B assumes a single episode of extraction of two crustal reservoirs from the mantle. These two reservoirs evolved toward the compositions of lead sources 1 and 2 respectively (Fig. 4B). Back-calculation indicates that this episode would have occurred at 3.65 Ga, which, in turn, imposes $\mu_1 = 11.12$ and $\mu_2 = 10.34$, and that Pb isotope evolution of lead source 1 would have ceased at 1764 Ma (i.e., was devoid of U and Th to avoid the production of radiogenic Pb). Model C assumes an initial extraction of a crustal reservoir from the mantle at 3.7 Ga, followed by an episode of differentiation into two crustal reservoirs that evolved toward the compositions of lead sources 1 and 2 respectively (Fig. 4C). Back-calculation indicates that crustal differentiation would have occurred between 3.65 and 3.0 Ga, which, in turn, imposes that Pb isotope evolution of lead source 1 would have ceased between 1895 and 1764 Ma, with μ_1 ranging between 11.12 and 12.92 and μ_2 ranging between 10.34 and 10.67.

Potential Candidates for Lead Sources

It is noteworthy that all scenarios require elevated μ values (between 10.2 and 12.92) for the crustal reservoirs in order to account for the compositions of lead sources 1 and 2, ruling out mafic volcanics from the McArthur Basin as a plausible Pb source for the McArthur River deposit (e.g., Stacey and Kramers, 1975; Cooke et al., 1998; Hofmann, 2007). Models B and C require that lead source 1 would have stopped evolving isotopically between ca. 1895 and 1764 Ma. This would be possible if lead source 1 consisted of galena or Pb-bearing feldspar crystallized within this age span. However, only small galena deposits of this age are known in the basin or basement in the area, and no felsic igneous rocks are recorded in the area between 1815 (oldest age in the basin) and 1730 Ma (Ahmad et al., 2013). Therefore, according to Model C, lead source 1 should belong to or be derived from the youngest basement felsic units by erosion and sedimentation. Lead sources 1 and 2 could actually belong to separate units, or to the same unit if, in the latter, Pb was alternatively

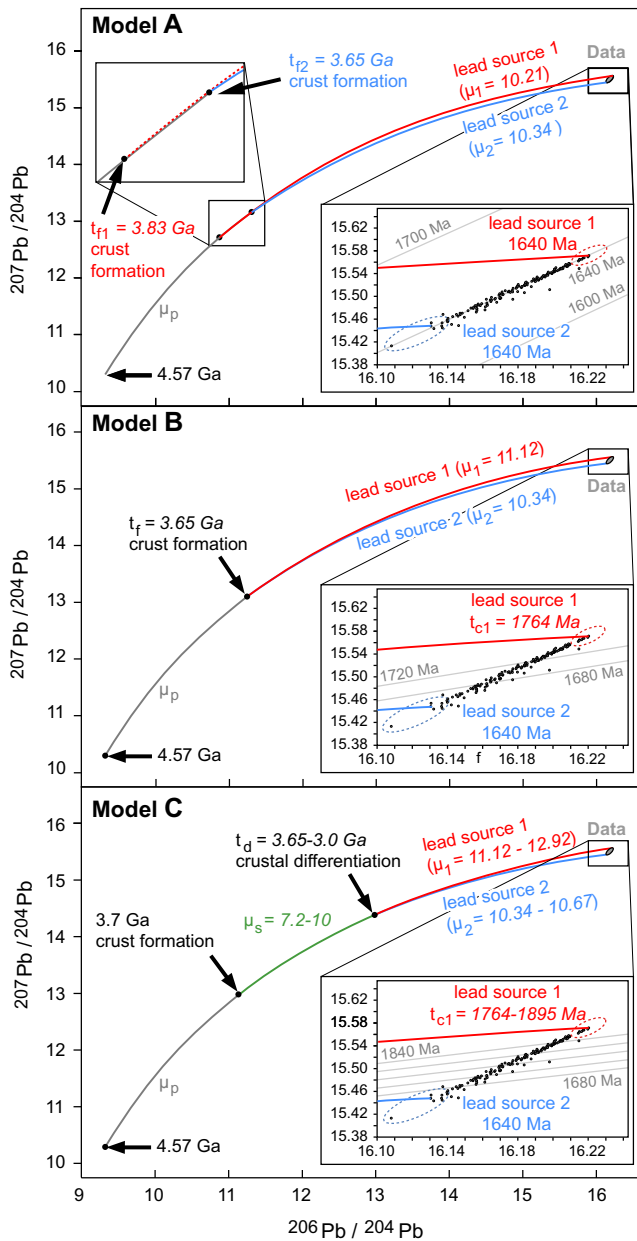


Figure 4. Lead isotope evolution models proposed for the origin of two lead sources in the McArthur River Zn-Pb deposit (Northern Territory, Australia). See text for description of models. The data presented are all the data obtained in this study. Colors in models A, B, and C: evolution of mantle—gray; lead source 1—red; lead source 2—blue; crustal reservoir formed prior to crustal differentiation (model C)—green. Isochrons (straight lines linking the compositions of rocks or minerals having the same model age) are indicated for each proposed model. Values in *italics* are calculated values after models. μ_p , μ_s , μ_1 , and μ_2 correspond to the $^{238}\text{U}/^{204}\text{Pb}$ ratio of mantle (7.192), first-formed crustal reservoir in model C, lead source 1, and lead source 2 respectively; t_1 and t_2 correspond to the age of crust formation for lead sources 1 and 2, respectively, in model A; t_1 and t_2 correspond to the ages of crust formation in model B and to episode of crustal differentiation after crust formation at 3.7 Ga in model C, respectively; t_{c1} is the time from which the isotopic composition of lead source 1 remained constant, corresponding to crystallization of Pb-bearing, U-poor and Th-poor minerals in models B and C.

leached from feldspar only or from all Pb-bearing minerals including accessory uranium- and thorium-rich minerals. Several anorogenic felsic intrusive and volcanic units in the crystalline basement are plausible candidates for lead sources 1 and 2 because they meet the age constraints from the above models and have vertical (>1 km) and lateral extents that could potentially account for the Pb budget of the McArthur River deposit (Table DR3). This includes the ca. 1850 Ma Cliffdale and Scrutton volcanics located in the Murphy and Scrutton inliers respectively (Fig. 1). Those anorogenic felsic units were likely among the sources of felsic-derived sediments in the McArthur Basin such as the black shales of the Barney Creek Formation, clastic units within carbonate-evaporite successions, or the regionally extensive and permeable conglomerates and sandstones in the basal units

of the McArthur Basin where framework alteration of detrital feldspar is documented (Davidson, 1998; Polito et al., 2011).

CONCLUSION

Altogether, our *in situ* SIMS Pb isotope data and isotope modeling provide, for the first time, a strong support for the previous assumption that the Pb-rich products of anorogenic felsic magmatism contributed to the Pb sources for some giant Proterozoic Zn-Pb deposits worldwide (Sawkins, 1989). More generally, our work shows that if forming a giant hydrothermal ore deposit requires mobilizing metals from several sources, the current models for scales, geometries, and dynamics of ore-forming hydrothermal systems should be revised. In turn, this would have a major impact on the estimation of metal endowment and exploration strategies in

world-class metallogenic provinces, because the volume of metal sources and their metal concentration define the total amount of metals available for ore deposits.

ACKNOWLEDGMENTS

The Northern Territory Geological Survey provided logistical support for sampling. Glencore Australia Holdings Pty Ltd and the McArthur River mine geologists team provided authorization and guidance for sampling. The Ion Probe Team Nancy (France; CRPG-CNRS) provided technical support during SIMS analyses. The Service Commun de Microscopie Electronique et de Microanalyses (GeoRessources laboratory, University of Lorraine, France) provided technical support during SEM analyses. This research was funded by (1) a French Ministry of Higher Education and Research Ph.D. salary grant to Gigon; (2) a Région Lorraine—FÉDER grant to Mercadier, “Rôle des phases fluides dans la distribution spatiale des ressources métalliques dans les bassins sédimentaires paléoproterozoïques australiens”; (3) Observatoire des Sciences de l’Univers (OSU) OTELO grants to Mercadier, “Conditions de transport des métaux dans un mégabassin protérozoïque”, and Richard, “Transferts de fluides et métaux dans le bassin de McArthur (Australie)”; and (4) CNRS-INSU-CESSUR grants to Mercadier “Transferts des fluides et métaux dans les méga-bassins paléoproterozoïques”, and Richard, “Traçage isotopique de migrations massives de métaux le long d’une faille d’échelle crustale (Emu Fault, bassin de McArthur, Australie)”. Reviews by Robert Scott and two anonymous reviewers greatly helped in improving the manuscript.

REFERENCES CITED

- Ahmad, M., Dunster, J.N., and Munson, T.J., 2013, McArthur Basin, in Ahmad, M., and Munson, T.J., compilers, *Geology and Mineral Resources of the Northern Territory: Northern Territory Geological Survey Special Publication 5*, p. 15–1–15–72.
- Cooke, D.R., Bull, S.W., Donovan, S., and Rogers, J.R., 1998, K-metasomatism and base metal depletion in volcanic rocks from the McArthur Basin, Northern Territory—Implications for base metal mineralization: *Economic Geology and the Bulletin of the Society of Economic Geologists*, v. 93, p. 1237–1263, <https://doi.org/10.2113/gsecongeo.93.8.1237>.
- Cooke, D.R., Bull, S.W., Large, R.R., and McGoldrick, P.J., 2000, The importance of oxidized brines for the formation of Australian Proterozoic stratiform sediment-hosted Pb-Zn (sedex) deposits: *Economic Geology and the Bulletin of the Society of Economic Geologists*, v. 95, p. 1–18, <https://doi.org/10.2113/gsecongeo.95.1.1>.
- Cumming, G.L., and Richards, J.R., 1975, Ore lead isotope ratios in a continuously changing earth: *Earth and Planetary Science Letters*, v. 28, p. 155–171, [https://doi.org/10.1016/0012-821X\(75\)90223-X](https://doi.org/10.1016/0012-821X(75)90223-X).
- Davidson, G.J., 1998, Alkali alteration styles and mechanisms, and their implications for a ‘brine factory’ source of base metals in the rift-related McArthur group, Australia: *Australian Journal of Earth Sciences*, v. 45, p. 33–49, <https://doi.org/10.1080/08120099808728365>.
- Deloule, E., Allegre, C.J., and Doe, B.R., 1986, Lead and sulfur isotope microstratigraphy in galena crystals from Mississippi Valley-type deposits: *Economic Geology and the Bulletin of the Society of Economic Geologists*, v. 81, p. 1307–1321, <https://doi.org/10.2113/gsecongeo.81.6.1307>.

- Harlaux, M., Mercadier, J., Marignac, C., Peiffert, C., Cloquet, C., and Cuney, M., 2018, Tracing metal sources in peribatholithic hydrothermal W deposits based on the chemical composition of wolframite: The example of the Variscan French Massif Central: *Chemical Geology*, v. 479, p. 58–85, <https://doi.org/10.1016/j.chemgeo.2017.12.029>.
- Hofmann, A.W., 2007, Sampling mantle heterogeneity through oceanic basalts: Isotopes and trace elements, in Carlson, R.W., ed., *Treatise on Geochemistry, Volume 2: The Mantle and Core: Elsevier*, 44 p., <https://doi.org/10.1016/B0-08-043751-6/02123-X>.
- Huston, D.L., Stevens, B., Southgate, P.N., Muhling, P., and Wyborn, L., 2006, Australian Zn-Pb-Ag ore-forming systems: A review and analysis: *Economic Geology and the Bulletin of the Society of Economic Geologists*, v. 101, p. 1117–1157, <https://doi.org/10.2113/gsecongeo.101.6.1117>.
- Kunzmann, M., Schmid, S., Blaikie, T.N., and Halverson, G.P., 2019, Facies analysis, sequence stratigraphy, and carbon isotope chemostratigraphy of a classic Zn-Pb host succession: The Proterozoic middle McArthur Group, McArthur Basin, Australia: *Ore Geology Reviews*, v. 106, p. 150–175, <https://doi.org/10.1016/j.oregeorev.2019.01.011>.
- Large, R.R., Bull, S.W., Cooke, D.R., and McGoldrick, P.J., 1998, A genetic model for the H.Y.C. Deposit, Australia: Based on regional sedimentology, geochemistry, and sulfide-sediment relationships: *Economic Geology and the Bulletin of the Society of Economic Geologists*, v. 93, p. 1345–1368, <https://doi.org/10.2113/gsecongeo.93.8.1345>.
- Laznicka, P., 2014, Giant metallic deposits—A century of progress: *Ore Geology Reviews*, v. 62, p. 259–314, <https://doi.org/10.1016/j.oregeorev.2014.03.002>.
- Leach, D.L., Bradley, D.C., Huston, D., Pisarevsky, S.A., Taylor, R.D., and Gardoll, S.J., 2010, Sediment-hosted lead-zinc deposits in Earth history: *Economic Geology and the Bulletin of the Society of Economic Geologists*, v. 105, p. 593–625, <https://doi.org/10.2113/gsecongeo.105.3.593>.
- McCuaig, T.C., and Hronsky, J.M.A., 2014, The mineral system concept: The key to exploration targeting, in Kelley, K.D., and Golden, H.C., eds., *Building Exploration Capability for the 21st Century: Society of Economic Geologists Special Publication 18*, p. 153–175, <https://doi.org/10.5382/SP.18.08>.
- McGoldrick, P., Winefield, P., Bull, S., Selley, D., and Scott, R., 2010, Sequences, synsedimentary structures, and sub-basins: The where and when of SEDEX zinc systems in the southern McArthur Basin, Australia, in Goldfarb, R.J., et al., eds., *The Challenge of Finding New Mineral Resources: Global Metallogeny, Innovative Exploration, and New Discoveries: Society of Economic Geologists Special Publication 15*, p. 367–390, <https://doi.org/10.5382/SP.15.2.02>.
- Mercadier, J., Annesley, I.R., McKechnie, C.L., Bogdan, T.S., and Creighton, S., 2013, Magmatic and metamorphic uraninite mineralization in the western margin of the Trans-Hudson orogen (Saskatchewan, Canada): A uranium source for unconformity-related uranium deposits?: *Economic Geology and the Bulletin of the Society of Economic Geologists*, v. 108, p. 1037–1065, <https://doi.org/10.2113/econgeo.108.5.1037>.
- NTGS (Northern Territory Geological Survey), 2019, Lead, zinc, silver factsheet and map: The Territory's Resources Commodities in the NT: https://resourcingtheterritory.nt.gov.au/_data/assets/pdf_file/0007/756556/LeadZincSilver-Factsheet.pdf (accessed January 2020).
- Page, R.W., and Sweet, I.P., 1998, Geochronology of basin phases in the western Mt Isa Inlier, and correlation with the McArthur Basin: *Australian Journal of Earth Sciences*, v. 45, p. 219–232, <https://doi.org/10.1080/08120099808728383>.
- Pettke, T., Oberli, F., and Heinrich, C.A., 2010, The magma and metal source of giant porphyry-type ore deposits, based on lead isotope microanalysis of individual fluid inclusions: *Earth and Planetary Science Letters*, v. 296, p. 267–277, <https://doi.org/10.1016/j.epsl.2010.05.007>.
- Pitcairn, I.K., Teagle, D.A.H., Craw, D., Olivo, G.R., Kerrich, R., and Brewer, T.S., 2006, Sources of metals and fluids in orogenic gold deposits: Insights from the Otago and Alpine schists, New Zealand: *Economic Geology and the Bulletin of the Society of Economic Geologists*, v. 101, p. 1525–1546, <https://doi.org/10.2113/gsecongeo.101.8.1525>.
- Polito, P.A., Kyser, T.K., Alexandre, P., Hiatt, E.E., and Stanley, C.R., 2011, Advances in understanding the Kombolgie Subgroup and unconformity-related uranium deposits in the Alligator Rivers Uranium Field and how to explore for them using litho-geochemical principles: *Australian Journal of Earth Sciences*, v. 58, p. 453–474, <https://doi.org/10.1080/08120099.2011.561873>.
- Rawlings, D.J., Korsch, R.J., Goleby, B.R., Gibson, G.M., Johnstone, D.W., and Barlow, M., 2004, The 2002 Southern McArthur Basin Seismic Reflection Survey: *Geoscience Australia Record 2004/17*, 87 p.
- Richard, A., Rozsypal, C., Mercadier, J., Banks, D.A., Cuney, M., Boiron, M.-C., and Cathelineau, M., 2012, Giant uranium deposits formed from exceptionally uranium-rich acidic brines: *Nature Geoscience*, v. 5, p. 142–146, <https://doi.org/10.1038/ngeo1338>.
- Richards, J.P., 2013, Giant ore deposits formed by optimal alignments and combinations of geological processes: *Nature Geoscience*, v. 6, p. 911–916, <https://doi.org/10.1038/ngeo1920>.
- Sawkins, F.J., 1989, Anorogenic felsic magmatism, rift sedimentation, and giant Proterozoic Pb-Zn deposits: *Geology*, v. 17, p. 657–660, [https://doi.org/10.1130/0091-7613\(1989\)017<0657:AFMRSA>2.3.CO;2](https://doi.org/10.1130/0091-7613(1989)017<0657:AFMRSA>2.3.CO;2).
- Stacey, J.S., and Kramers, J.D., 1975, Approximation of terrestrial lead isotope evolution by a two-stage model: *Earth and Planetary Science Letters*, v. 26, p. 207–221, [https://doi.org/10.1016/0012-821X\(75\)90088-6](https://doi.org/10.1016/0012-821X(75)90088-6).
- Sun, S.s., Carr, G.R., and Page, R.W., 1996, A continued effort to improve lead-isotope model ages: *Australian Geological Survey Organization Research Newsletter*, v. 24, p. 19–20.

Printed in USA